Mechanism of unidirectional motions of chiral molecular motors driven by linearly polarized pulses

ARTICLE *in* THE JOURNAL OF CHEMICAL PHYSICS · DECEMBER 2003

Impact Factor: 2.95 · DOI: 10.1063/1.1621622

4 AUTHORS, INCLUDING:

Kunihito Hoki
The University of Electro-Communications
51 PUBLICATIONS **737** CITATIONS
SEE PROFILE

Yuichi Fujimura
Tohoku University
227 PUBLICATIONS **3,268** CITATIONS
SEE PROFILE

Mechanism of unidirectional motions of chiral molecular motors driven by linearly polarized pulses

Kunihito Hoki and Masahiro Yamaki
Department of Chemistry, Graduate School of Science, Tohoku University, Sendai 980-8578, Japan

Shiro Koseki
Department of Material Science, College of Integrated Arts and Sciences, Osaka Prefecture University, Sakai, Osaka 599-8531, Japan

Yuichi Fujimura[a)]
Department of Chemistry, Graduate School of Science, Tohoku University, Sendai 980-8578, Japan

(Received 28 April 2003; accepted 3 September 2003)

The mechanism of the unidirectional rotational motion of a chiral molecular motor driven by linearly polarized laser pulses was theoretically studied. A simple aldehyde molecule was adopted as a chiral molecular motor, in which a formyl group (–CHO) was the rotating part of the motor. Temporal evolutions of the instantaneous angular momentum averaged over an ensemble of randomly oriented motors were taken as a measure of the unidirectional motion. The contour plots of the averaged instantaneous angular momentum were obtained by using a quantum master equation approach that took into account relaxation effects and a classical trajectory approach. Two regimes are found in the contour plots. One is an intense laser field regime in which the laser–motor interaction energy exceeds the asymmetric potential barrier. In this regime, the motors are unidirectionally driven in the intuitive direction, i.e., the gentle slope of the potential. The other regime is a subthreshold laser intensity regime in which unintuitive rotational motions also occur. This unintuitive rotation is found to be a quantum effect, as indicated by contour plots calculated by taking into account temperature effects. © *2003 American Institute of Physics.*
[DOI: 10.1063/1.1621622]

I. INTRODUCTION

In recent years, there has been increased interest in the study of molecular motors due to their important applications to the design of nanostructured devices.[1–5] Koumura *et al.* reported interesting results of experiments on molecular motors.[6,7] Their molecular motors were constructed from chiral aromatic compounds, and *cis–trans* photoisomerizations of the compounds induced by both linearly polarized incoherent UV (vacuum ultraviolet) lights and thermal energy were the origin of unidirectional motion. Much interest has been shown in chiral molecular motors driven by laser pulses since such motors can in principle be controlled by using laser pulses. In previous studies, we clarified the roles of molecular chirality and photon helicity in determination of unidirectional rotation.[8] A linearly polarized laser pulse with a strong intensity can rotate a chiral molecular motor in an intuitive way. Here intuitive rotation means that the direction of rotation is toward a gentle slope of the asymmetric potential of a chiral molecule. We have also shown that the motor actions consist of a sequence of pendulum and true rotational motions after ignition of the motor by applying a laser pulse.[9]

Several issues regarding chiral molecular motors driven by laser pulses remain to be clarified. One issue is related to the mechanisms of unidirectional motion of chiral molecular motors. It is well known that time-correlated forces $f(t)$ can unidirectionally drive a ratchet system with asymmetric potential.[10] An example of so-called Brownian motors is shown in the upper panel of Fig. 1. Here, the time-dependent effective potential $V(x,t)$ consisting of ratchet potential $V_0(x)$ and an interaction potential, $xf(t)$ is schematically shown. The effective potential is characterized by a nonperiodic coordinate-dependence. On the other hand, the lower panel of Fig. 1 shows time-dependent effective potential in which the interaction potential is of a periodic nature. This corresponds to a chiral molecular motor driven by linearly polarized laser pulses. The unidirectional motion cannot simply be explained from this figure because linearly polarized laser pulses shake the asymmetric potential up and down.

Furthermore, we found from contour plots of time evolutions of instantaneous angular momentum that chiral molecular motors can rotate unintuitively as well as intuitively in the case in which the applied laser is in the regime of a subthreshold intensity. The origin of such unintuitive rotations is not known.

Another issue is related to environmental effects. In our previous studies, we used an idealized model for molecular motors, in which environmental effects were not considered.[8,9] Environmental factors have significant effects on molecular motors. Analysis of environmental effects from a microscopic point of view provides information on the mechanism by which kinetic energy of the motor is con-

a)Author to whom all correspondence should be addressed; electronic mail: fujimura@mcl.chem.tohoku.ac.jp

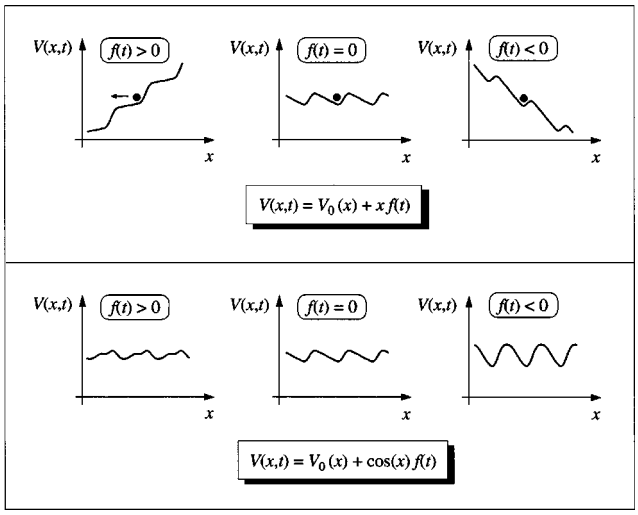

FIG. 1. Two types of time-dependent effective potential $V(x,t)$. The potential consists of a ratchet potential $V_0(x)$ and an interaction potential. In the upper panel, the interaction potential is a nonperiodic one, for simplicity, given by $xf(t)$. Here, $f(t)$ is a time-dependent term. Brownian motors are driven by such a nonperiodic interaction potential. In the lower panel, the interaction potential is a periodic one. A chiral molecular motor driven by a linearly polarized laser pulse is explained in terms of such a periodic interaction (see Fig. 4).

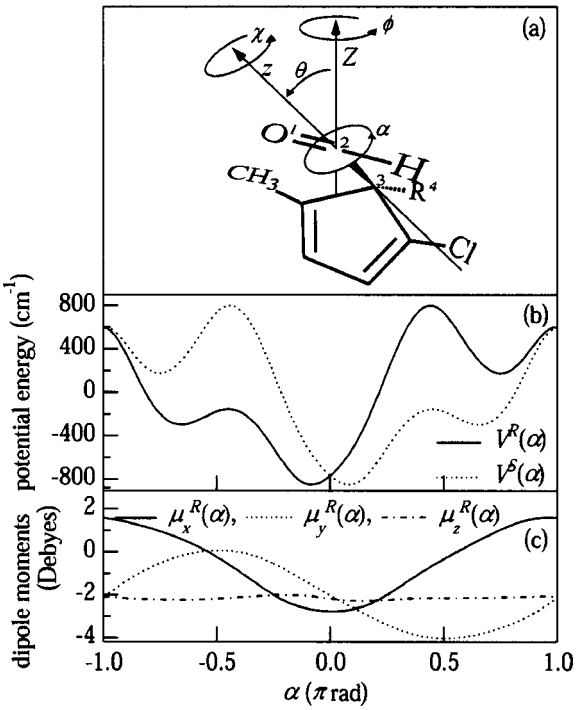

FIG. 2. (a) A chiral molecular motor with internal rotational coordinate α of a CHO group and Euler angles $\Omega(\phi,\theta,\chi)$. The Euler angles define the orientation in space of the main part of the molecule that includes a five-membered ring. In this figure, $-R^4$ represents an alkyl group. (b) Potential energies calculated as a function of α of (*S*) and (*R*) motors. Here, a hydrogen atom is substituted for the alkyl group $-R^4$. (c) Dipole moments of the (*R*) motor.

verted into heat. So far, environmental effects have been studied mainly by using methods of classical molecular dynamics simulations. Vacek and Michl carried out dynamics simulations of a molecular propeller mounted in the center of a square grid that was exposed to a flow of a rare gas from a supersonic nozzle.[11] Space *et al.*, showed the feasibility of creating a measurable concentration gradient of propeller molecules in a solvent by a laser driven photophoresis process by using molecular dynamics simulation.[12]

In this paper, we focus on the mechanisms of unidirectional motions of chiral molecular motors driven by linear polarized laser pulses. In Sec. II, we briefly describe a theoretical method; the instantaneous angular momentum averaged over an ensemble of randomly oriented motors is derived from a quantum master equation approach that takes into account environmental effects. In Sec. III, we present contour plots of the instantaneous angular momentum to show how unidirectional motions depend on laser intensity and central frequency. We discuss the mechanism of unidirectional motions in terms of a rotational wave packet created by intense laser pulses. Two regimes were found in the contour plots: an intense laser field regime and a subthreshold laser intensity regime. In the intense laser field regime, the laser–motor interaction energy exceeds the asymmetric potential barrier. The motors are unidirectionally driven in the intuitive direction. In the subthreshold laser intensity regime, unintuitive rotational motions due to a quantum effect occur.

II. THEORY

As a model system of a real quantum molecular motor, we selected a chiral aldehyde molecule shown in Fig. 2(a). The internal rotation of the formyl group CHO around the C^2-C^3 bond is characterized by an asymmetric potential energy as shown in Fig. 2(b). The dihedral angle between the $O^1-C^2-C^3$ and $C^2-C^3-R^4$ planes is the dynamical variable for the motor.

The model system has the essential properties of a typical molecular motor; that is, the potential energy surface is asymmetric, and the dipole moment vector varies to some extent along the dihedral angle because of the electronegativity of the O^1 atom.[8] Rotational constants of the whole molecule are of the order of a few GHz (see Sec. III). Since the energy spectrum of whole molecular rotation is dense compared to that of the internal rotation, we consider a situation in which the whole molecular rotational state is expressed in terms of a mixed state consisting of many rotational levels. Under this situation, the whole molecular rotation can be treated based on classical statistics. Effects of the molecular rotation within several tens of picoseconds can be ignored under low temperature conditions, or molecular motors are considered to be isotropically imbedded in a glass in a way that does not prevent the aldehyde group from turning freely. Since we ignore the molecular rotations, we chose the axis of internal rotation rather than the principal axis of the moment of inertia as the z axis in a molecular fixed frame.

The coordinates of the motor are defined in Fig. 2(a), where the Z axis is the direction of the electric field in a spatially fixed frame. The Hamiltonian of the molecular motor in the electric field of the laser $\mathbf{E}(t)$ is expressed within the semiclassical representation of matter and radiation field interactions as

$$H^{\xi}(t) = -\frac{\hbar^2}{2I}\frac{\partial^2}{\partial\alpha^2} + V^{\xi}_{\mathrm{eff}}(t) \quad (\xi = S \text{ or } R). \tag{1}$$

Here, I is the moment of inertia of the molecular motor. Effective interaction $V^{\xi}_{\mathrm{eff}}(t)$ is expressed within the dipole approximation as

$$V^{\xi}_{\mathrm{eff}}(t) = V^{\xi}(\alpha) - \boldsymbol{\mu}^{\xi}(\alpha)\cdot\mathbf{E}(t), \tag{2}$$

where $V^{\xi}(\alpha)$ is the asymmetric potential energy function of the molecular motor, and $\boldsymbol{\mu}^{\xi}(\alpha)$ is the dipole moment vector. The inner product, $\boldsymbol{\mu}^{\xi}(\alpha)\cdot\mathbf{E}(t)$, depends on the Euler angles $\Omega(\phi,\theta,\chi)$. The asymmetry in the potential originates from molecular chirality, for example, *S* or *R*. The superscript ξ is explicitly indicated in Eqs. (1) and (2) since nuclear motions associated with chiral change are not taken into account and the internal rotation is defined within each chiral molecule. In this paper, we call a molecular motor constructed from an (*S*) enantiomer and that constructed from an (*R*) enantiomer an (*S*) motor and (*R*) motor, respectively.

Consider that the motor system interacts with bath *B* and that the total Hamiltonian is described by

$$H^{\xi}_{T}(t) = H^{\xi}(t) + H_B + H^{\xi}_{I}, \tag{3}$$

where H_B is the Hamiltonian of bath *B*, and H^{ξ}_{I} is the interaction between the system and bath *B*. We assume that the system and the bath are separable. Within this approximation, dynamics of the motor system is described by its reduced density matrix $\rho^{\xi}(t)$ that is obtained from the total density matrix $\rho^{\xi}_{T}(t)$ by taking the trace over the bath variables as $\rho^{\xi}(t) = \mathrm{Tr}_B\{\rho^{\xi}_{T}(t)\}$.

In this paper, we adopt a Lindblad-type equation as the equation of motion of the reduced density operator $\rho^{\xi}(t)$,[13,14]

$$i\hbar\frac{\partial}{\partial t}\rho^{\xi}(t) = [H^{\xi}(t),\rho^{\xi}(t)] + \frac{i}{2}\sum_{n}\{[A^{\xi}_{n}\rho^{\xi}(t),A^{\xi\dagger}_{n}] + [A^{\xi}_{n},\rho^{\xi}(t)A^{\xi\dagger}_{n}]\}. \tag{4}$$

The above differential equation has desirable properties as an equation of motion of the density operator. That is, (i) Eq. (4) is linear for $\rho^{\xi}(t)$, (ii) $\rho^{\xi}(t)$ retains essential properties of the density operator: Hermitian, positive definite, and trace is equal to unity, and (iii) Eq. (4) has a semi-group property of the type $i\hbar(d/dt)\rho^{\xi}(t) = \mathcal{L}^{\xi}\rho^{\xi}(t)$, where $\mathcal{L}^{\xi}$ is a linear mapping of operators.

The initial state $\rho^{\xi}(t=0)$ is in thermal equilibrium, that is, the canonical distribution without electric field at temperature *T*. The time-dependent Hamiltonian and the states satisfy the periodical boundary condition of 2π. The second term in the right-hand side of Eq. (4) denotes the relaxation effects originating from interactions between motors and bath modes of their environment. In this paper, we set the interaction operator A^{ξ}_{n} to $|n+1\rangle^{\xi}a_n{}^{\xi}\langle n| + |n\rangle^{\xi}b_n{}^{\xi}\langle n+1|$, $(n=0,1,...)$. Only inelastic scattering processes were taken into account and elastic interactions were ignored. Here, to qualitatively discuss relaxation effects, both the interaction parameters a_n and b_n were assumed to be given by

$$\frac{a_n^2}{b_n^2} = \exp\left(-\frac{E_{n+1}-E_n}{kT}\right), \quad \text{and} \quad a_n^2 + b_n^2 = \frac{\hbar}{\tau_0}\frac{E_{n+1}-E_0}{E_1-E_0},$$

in which E_n denotes the *n*th eigenstate of the quantum motor, and τ_0 is relaxation time from $n=1$ to 0. This is a simple extension of the two-state model to the multistate system of the motor. The quantum master equation, Eq. (4), was solved by means of the split operator and a finite difference method with a fast Fourier transform algorithm using 256 grids for α.

In order to quantitatively discuss the dynamics of molecular motors in a quantum mechanical way, we now introduce an angular momentum operator of the internal rotation $-i\hbar(\partial/\partial\alpha)$. An expectation value of the angular momentum operator at time *t*, $l^{\xi}(t)$, is defined as

$$l^{\xi}(t) = \int_{-\pi}^{\pi}d\alpha'\int_{-\pi}^{\pi}d\alpha\left\{-i\hbar\frac{\partial\delta(\alpha'-\alpha)}{\partial\alpha}\rho^{\xi}(\alpha,\alpha',t)\right\}, \tag{5}$$

where $\rho^{\xi}(\alpha,\alpha',t)$ denotes $\rho^{\xi}(t)$ in the coordinate representation. In this paper, $l^{\xi}(t)$ is called the instantaneous angular momentum.

The instantaneous angular momentum of an ensemble of randomly oriented motors, $\langle l^{\xi}(t)\rangle$, is expressed by averaging $l^{\xi}(t)$ over all of the Euler angles $\Omega(\phi,\theta,\chi)$ as

$$\langle l^{\xi}(t)\rangle_{\Omega} = \frac{1}{8\pi^2}\int_0^{2\pi}d\phi\int_0^{\pi}d\theta\int_0^{2\pi}d\chi\, l^{\xi}(t)\sin\theta. \tag{6}$$

The linearly polarized electric field has a symmetry around the *Z* axis or Euler angle ϕ. Twofold integral calculus was carried out by using the trapezoidal rule with 16 grid points for θ and 64 grid points for χ.

III. RESULTS AND DISCUSSION

In order to accurately evaluate properties of chiral molecular motors, we selected 2-methyl-cyclopenta-2,4-dienecarbaldehyde, in which a hydrogen atom is substituted for the alkyl group, -R, shown in Fig. 2(a).[15] Rotational constants of the whole molecule are 1.97, 1.16, and 0.79 GHz.[8] The potential energies and dipole moments of the chiral molecular motor were calculated using the GAUSSIAN 98 package of programs.[16] The 6-31G(*d*) basis set in the MP2 method was used. The potential energy was calculated at every dihedral angle, $O^1-C^2-C^3-H^4$, while all of the other internal coordinates were fully optimized. Figure 2(c) shows the three components of the dipole moment vector as a function of α, which were calculated in the molecular fixed Cartesian coordinates *xyz*. Here the *z* axis is set to be heading from C^3 to C^2, and the *x* axis is set to be heading to H^4 and is at a right angle to the *z* axis. We note from a symmetric consideration that those *x* and *y* components are expressed in a good approximation by a sinusoid function, i.e., $\boldsymbol{\mu}^{S}(\alpha) = \mu\cos(\alpha)\mathbf{e}_x - \mu\sin(\alpha)\mathbf{e}_y$ for the (*S*) motor and $\boldsymbol{\mu}^{R}(\alpha) = -\mu\cos(\alpha)\mathbf{e}_x - \mu\sin(\alpha)\mathbf{e}_y$ for the (*R*) motor. Here, μ is nearly 2 D, the internal rotation axis is parallel to the molecular fixed *z* axis, and $\mathbf{e}_x$ and $\mathbf{e}_y$ are unit vectors of *x* and *y*, respectively.

Figure 3 shows the temporal behaviors of the instantaneous angular momentum $\langle l^{R}(t)\rangle_{\Omega}(\langle l^{S}(t)\rangle_{\Omega})$ of the (*R*) ((*S*))

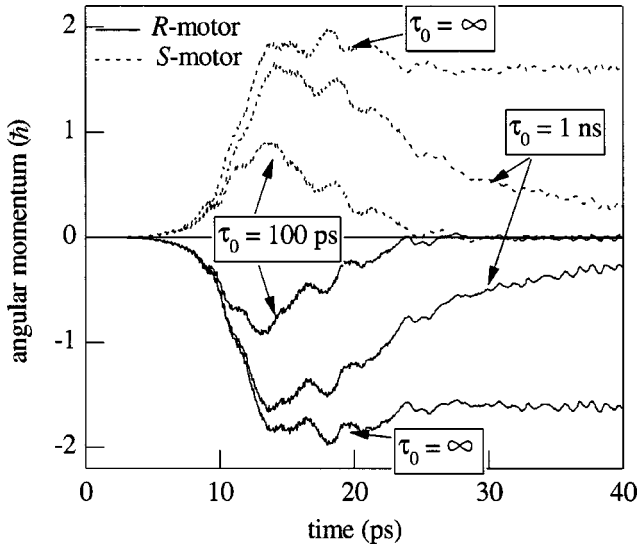

FIG. 3. Temporal behaviors of the instantaneous angular momentum of randomly oriented (R) motors, $\langle l^R(t)\rangle_\Omega$, denoted by a solid line, and those of (S) motors, $\langle l^S(t)\rangle_\Omega$, denoted by a dotted line at $T=150$ K. τ_0 denotes the relaxation time from the first excited state ($n=1$) to the lowest state ($n=0$).

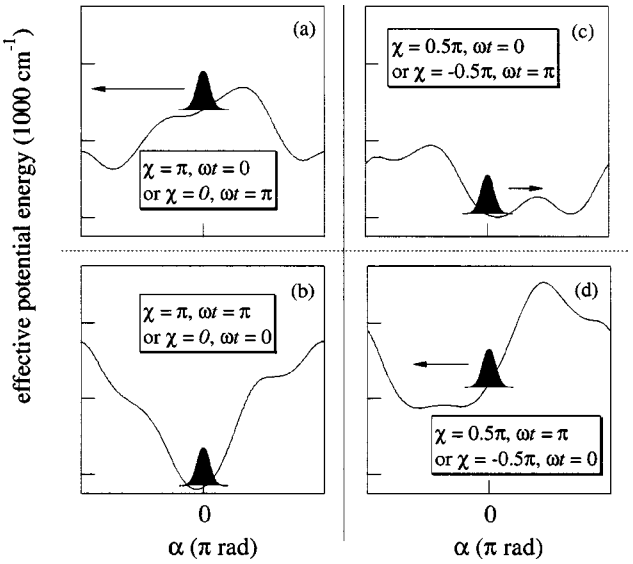

FIG. 4. A schematic view of a localized rotational wave packet on the effective potential energy function of the (R) motor fixed at specified Euler angle χ and time ωt. The effective potential is constructed from the internal rotation potential and the time-dependent periodic interaction of the chiral motor.

motors in the case in which there exist relaxation processes. For comparison, the temporal behaviors of $\langle l^R(t)\rangle_\Omega(\langle l^S(t)\rangle_\Omega)$ in the case in which there is no relaxation process are shown as well. The electric field of the laser pulse is: $\boldsymbol{E}(t)=f(t)\cos(\omega t)\mathbf{e}_Z$ for $0\leqslant t\leqslant t_f$ and $\boldsymbol{E}(t)=0$ for $t_f<t$. Here, $t_f=30$ ps, its central frequency ω is set to be 2.34×10^{13} rad/s ($124\,\mathrm{cm}^{-1}$), and pulse envelope function $f(t)$ is set to be $E_0\sin^2(\pi t/t_f)$ with $E_0=3.4$ GV/m. We can see that unidirectional rotational motion is maintained even if the laser pulse is turned off in the case in which there is no relaxation process. This means that a part of time-dependent density forms a rotating wave packet.[8] It should be noted that the rotational direction of the (S) motor is opposite to that of the (R) motor and the direction of rotation of both the motors is toward the gentle slope of each potential. This indicates that the direction of rotation of motors can be controlled by changing molecular chirality.[17,18]

Figure 3 also shows the effects of relaxation on $\langle l^\xi(t)\rangle_\Omega$. The relaxation time from the first excited state to the ground state, τ_0, was taken to be a relaxation parameter. In these simulations, we ignored ultrafast inertial effects, assuming that the modeled system was weakly fluctuating. Such a situation can be realized in the case in which motors are surrounded by solvent cage molecules or imbedded in a rigid solvent under low temperature conditions.[19] It is well known that internal rotation of a substituent that is chemically bonded to an aromatic ring of a molecule is subjected to relaxation due to inelastic interactions between its substituent and solvents or intramolecular interactions in a solvent. The magnitudes of such relaxations have been measured by spectroscopic techniques such as electron spin resonance.[20] In Fig. 3, we can see strong dependence on τ_0. This is mainly because effective relaxation times were taken to be proportional to the excess energy of the internal rotation in the present relaxation model. Therefore, the magnitude of the effective relaxation time in the 54th quantum state just over barrier height V_0 is shorter than that of τ_0 by about two orders of magnitude, for example, ~5 ps for $\tau_0=100$ ps. One of the methods for continuously driving molecular motors under such a relaxation condition is to sequentially apply intense laser pulses to the motor in order to recover the rotational energy loss and accelerate the rotation. The results shown in Fig. 3 were obtained by application of only one intense pulse.

Figure 4 shows the effective potential and rotational wave packets of the (R) motor at several Euler spatial configurations to qualitatively understand its unidirectional motion. The creation of rotational wave packets and detailed analysis of their time evolution are discussed elsewhere.[21] The Euler angle θ was set to be 0.5π, which gives the maximum overlap between the dipole moment vector and the photon polarization. The amplitude of the electric field was set to be the same as that in Fig. 3. The rotational wave packet was initially localized around the stable configuration, $\alpha\simeq0$. It can be seen from Fig. 4 that the initial rotational wave packet at the configuration $\chi=0$ at $\omega t=\pi$ or $\chi=\pi$ at $\omega t=0$ moves toward the left-hand side with a gentle slope when the wave packet is shaken by a strong pulsed laser. On the other hand, Figs. 4(c) and 4(d) show that the rotational wave packet shaken by a pulsed laser at the configuration $\chi=\pm0.5\pi$ cannot obtain sufficient angular momentum to cross the potential barrier after the laser pulse is turned off. The origin of the unidirectional motion is the asymmetry of the rotational potential. The laser acts as an accelerator of the molecular motor. The initial angular momentum is large enough to determine the rotation toward the gentle slope of the rotational potential after the application of the laser pulse.

We now examine the dependence of ω and E_0 on the molecular motors. Figure 5 shows contours of the angular

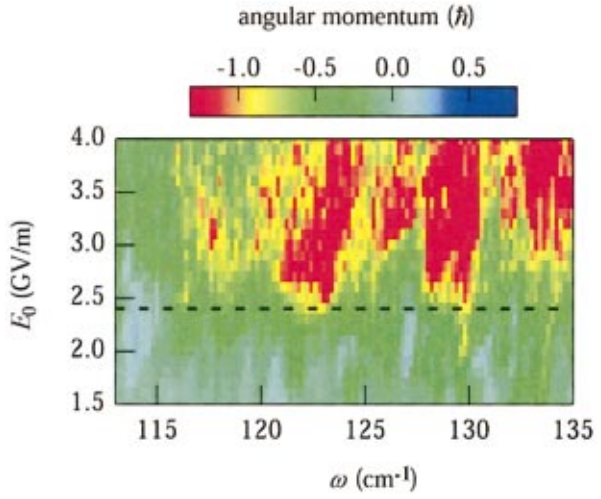

FIG. 5. (Color) Contour plots of the angular momentum in units of $\hbar$ of randomly oriented (R) motors $\langle l^R(t)\rangle_\Omega$ as a function of central frequency ω and amplitude E_0 of a laser pulse at $t=30$ ps and at $T=150$ K. The same envelope form of the electric field as that of previous one, $f(t)$, is adopted. The broken line denotes a threshold dividing intuitive and nonintuitive rotations. The red zone above the dividing line indicates highly intuitive rotations.

momentum at $t=30$ ps in the case in which there is no relaxation process. In Fig. 5, the absolute values of the angular momentum larger than $\sim 0.1\ \hbar$, which mainly result from averaging over orientations of motors, are persistent and not due to instantaneous fluctuations because such absolute values can be seen at a time longer than 30 ps. It can be seen in Fig. 5 that the contours can be divided into two regions. Its dividing line is denoted by a broken line. There also exists such a dividing line in other time domains. The critical value of E_0 is nearly 2.4 GV/m, which corresponds to the laser–motor interaction energy whose magnitude is 1650 cm^{-1}. The interaction energy is equal to V_0 to a good approximation. In the region above the dividing line, the sign of the greater part of the angular momentum $\langle l^R(t)\rangle_\Omega$ is negative, i.e., motors rotate toward the gentle potential energy side. In this region, the magnitude of the laser–motor interaction is greater than that of the internal rotational potential barrier $2\mu E_0 > V_0$, ensuring nonresonant forced rotation. On the other hand, in the region below the dividing line, unintuitive,

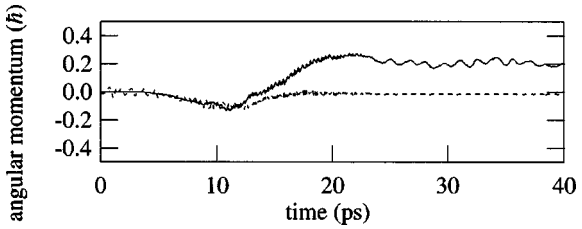

FIG. 6. Temporal behaviors of (R) motors in a regime of medium intensity in which $2\mu E_0 < V_0$ is satisfied. Here, $E_0=2.2$ GV/m and $\omega=114.0$ cm^{-1}. The other parameters are the same as those in Fig. 3. The solid line denotes $\langle l^R(t)\rangle_\Omega$ calculated using the quantum master equation, and the dotted line denotes $\langle l^R(t)\rangle_\Omega$ calculated using classical mechanics. The solid line indicates unintuitive rotation, while the dotted line indicates no rotation after the laser pulse is turned off.

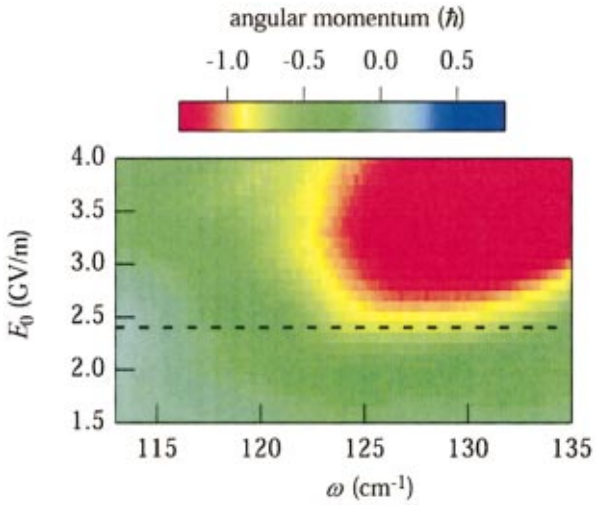

FIG. 7. (Color) Contour plots of the angular momentum in units of $\hbar$ of randomly oriented (R) motors $\langle l^R(t)\rangle_\Omega$ at $T=150$ K, which were calculated using classical mechanics.

reverse rotations toward the steeper potential energy side occur, although the initial angular rotation is toward the gentle side as shown in Fig. 6.

Figure 6 shows temporal behaviors of (R) motors in a regime of medium laser intensity, $2\mu E_0 < V_0$. We can see in Fig. 6 that reverse rotations, i.e., unintuitive rotations, occur just after the transient forward rotation around the pulse peak condition at 15 ps. This type of unintuitive motion is due to a quantum effect. To clarify this, contour plots of the angular momentum based on classical mechanics are also shown in Fig. 7, where $\langle l^R(t)\rangle_\Omega$ was obtained by solving the classical equation of motions. Here, for simplicity, relaxation effects were omitted. The initial distribution was set to be a canonical distribution at temperature $T=150$ K. The results of the classical treatment show that there is no unidirectional rotation under the same condition as that used in solving the quantum master equation with $\tau_0=\infty$. On the other hand, the

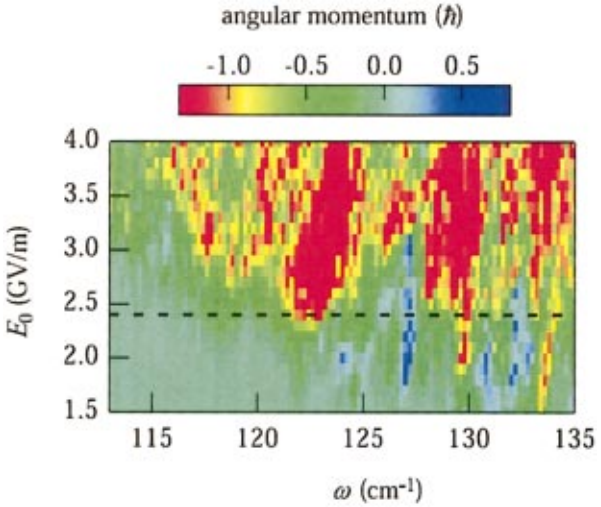

FIG. 8. (Color) Contour plots of the angular momentum in units of $\hbar$ of randomly oriented (R) motors $\langle l^R(t)\rangle_\Omega$ at $T\sim 0$ K, which were quantum mechanically calculated.

same intuitive rotation as that obtained by the quantum master equation is reproduced in the case in which condition $2\mu E_0 > V_0$ is satisfied, as can be seen in Fig. 7. If there is no relaxation effect, the unintuitive rotation persists after the laser pulse is turned off. In the presence of relaxation processes, e.g., in the case of $\tau_0 = 100$ ps, the rotation disappears at $t = 20$ ps, which is similar to that shown in Fig. 3. The quantum behaviors are diminished because the magnitudes of $\langle l^R(t)\rangle_\Omega$ are small compared with those in the intuitive case shown in Fig. 3 by a factor of 6–8. Therefore, to observe such quantum behaviors, the molecular system should be placed under a condition in which the relaxations have no significant contribution.

Results of simulations of temperature dependence on contour plots of angular momentum further support the speculation that unintuitive motions are due to quantum effects in a regime of medium laser intensity. Figure 8 shows the contour plots quantum mechanically calculated under low temperature conditions at $T \sim 0$ K, where the initial density operator is expressed in terms of the pure ground internal rotational state $|0\rangle\langle 0|$. Here we notice that area of unintuitive motions increases in size compared with those at $T = 150$ K shown in Fig. 5.

In summary, we have clarified the mechanism of unidirectional motion of randomly oriented chiral molecular motors driven by linearly polarized laser pulses by analyzing the contour plots of the instantaneous angular momentum averaged over their orientations. The instantaneous angular momentum was estimated by using a quantum master equation approach and a classical approach of a trajectory calculation. The internal rotation of a chiral aldehyde molecule was considered as a simple system of a chiral molecular motor, in which a formyl group (–CHO) was the rotating part of the motor. In an intense laser field regime, unidirectional rotational motion occurs in the intuitive direction of the gentle potential side. In a subthreshold laser intensity regime, an unintuitive rotational motion, which is due to quantum effects, occurs. Such unidirectional motions have qualitatively been explained in terms of rotational wave packets on the effective potential created by an intense laser pulse: the wave packet is impulsively rocking up and down by linearly polarized intense pulses and driven in an intuitive manner. In a sub-intensity regime, the wave packet may split into two parts: one that moves in an intuitive direction and the other that moves in an unintuitive direction.

Finally, it should be noted that the kinetic energy of unidirectional rotation created by a laser pulse was directly converted to thermal energy through motor–bath couplings without any work. The possibility of converting the kinetic energy of motors into that of other systems, e.g., propelling molecules, should be considered in future works. The possibility of converting the kinetic energy into potential energies of other molecular systems, bringing about a change in the shapes or assemblies of the systems, should also be considered.

ACKNOWLEDGMENTS

This work was partly supported by a Grant-in-aid for Scientific Research on Priority Areas ''Control of Molecules in Intense Laser fields'' (Area No. 419) and by a Grant-in-Aid for Scientific Research (No. 1555002) from the Ministry of Education, Culture, Sports, Science and Technology of Japan. K.H. acknowledges support from a Research Fellowship of the JSPS (No. 6254).

[1] F. Jülicher, A. Ajdari, and J. Prost, Rev. Mod. Phys. **69**, 1269 (1997).
[2] V. Balzani, M. G.-López, and J. F. Stoddart, Acc. Chem. Res. **31**, 405 (1998).
[3] *Molecular Machines and Motors*, edited by J.-P. Sauvage (Springer, Berlin, 2001).
[4] R. E. Tuzun, D. W. Niod, and B. G. Sumpter, Nanotechnology **6**, 52 (1995).
[5] J. Vacek and J. Michl, Proc. Natl. Acad. Sci. U.S.A. **98**, 5481 (2001).
[6] N. Koumura, R. W. J. Zijlstra, R. A. van Delden, N. Harada, and B. L. Feringa, Nature (London) **401**, 152 (1999).
[7] B. L. Feringa, N. Koumura, R. A. van Delden, and M. K. J. ter Wiel, Appl. Phys. A: Mater. Sci. Process. **75**, 301 (2002).
[8] K. Hoki, M. Yamaki, S. Koseki, and Y. Fujimura, J. Chem. Phys. **118**, 497 (2003).
[9] K. Hoki, M. Yamaki, and Y. Fujimura, Angew. Chem., Int. Ed. Engl. **42**, 2976 (2003).
[10] M. O. Magnasco, Phys. Rev. Lett. **71**, 1477 (1993); C. R. Doering, W. Horsthemke, and J. Riordan, *ibid.* **72**, 2984 (1994); R. Bartussek, P. Hänggi, and J. G. Kissner, Europhys. Lett. **28**, 459 (1994); R. D. Astumian, Science **276**, 917 (1997); R. Roncaglia and G. P. Tsironis, Phys. Rev. Lett. **81**, 10 (1998); H. Qian, *ibid.* **81**, 3063 (1998); M. B. Tarlie and R. D. Astumian, Proc. Natl. Acad. Sci. U.S.A. **95**, 2039 (1998); Y. Aghababaie, G. I. Menon, and M. Plischke, Phys. Rev. E **59**, 2578 (1999); M. Porto, M. Urbakh, and J. Klafter, Phys. Rev. Lett. **85**, 491 (2000); R. Lipowsky, *ibid.* **85**, 4401 (2000); G. Lattanzi and A. Maritan, *ibid.* **86**, 1134 (2001); M. Porto, Phys. Rev. E **63**, 030102 (2001); C. J. Olson, C. Reichhardt, B. Jankó, and F. Nori, Phys. Rev. Lett. **87**, 177002 (2001).
[11] J. Vacek and J. Michl, New J. Chem. **21**, 1259 (1997).
[12] B. Space, H. Rabitz, A. Lörincz, and P. Moore, J. Chem. Phys. **105**, 9515 (1996).
[13] G. Lindblad, Commun. Math. Phys. **48**, 119 (1976).
[14] N. G. van Kampen, *Stochastic Processes in Physics and Chemistry*, Revised and enlarged edition (North-Holland, Amsterdam, 1992), Chap. XVII.
[15] This molecule in solvents is known to be racemized due to keto-enol tautomerization in ordinary experimental conditions. Therefore, from an experimental point of view, another molecule, for example, a molecule in which the alkyl group is replaced by a methyl group instead of hydrogen, should be adopted as a chemically stable motor.
[16] M. J. Frisch, G. W. Trucks, H. B. Schlegel *et al.*, GAUSSIAN98 (RevisionA.7) Gaussian, Inc., Pittsburgh, PA (1998).
[17] M. Shapiro, E. Frishman, and P. Brumer, Phys. Rev. Lett. **84**, 1669 (2000).
[18] K. Hoki, L. González, and Y. Fujimura, J. Chem. Phys. **116**, 8799 (2002).
[19] *Rotational Dynamics of Small and Macromolecules*, edited by T. Dorfmüller and R. Pecora (Springer, Berlin, 1987).
[20] I. Miyazawa and K. Itoh, J. Chem. Phys. **36**, 2157 (1962).
[21] K. Hoki, M. Sato, M. Yamaki, R. Sahnoun, L. González, S. Koseki, and Y. Fujimura (unpublished).